Paper Presentation

Vivek Yadav
(CY20D751)

ADVANCED MATERIALS

Research Article | Full Access

Nanocluster Surface Microenvironment Modulates Electrocatalytic CO_2 Reduction

Seungwoo Yoo, Suhwan Yoo, Guocheng Deng, Fang Sun, Kangjae Lee, Hyunsung Jang, Chan Woo Lee, Xiaolin Liu, Junghwan Jang, Qing Tang ✉, Yun Jeong Hwang ✉, Taeghwan Hyeon ✉, Megalamane Siddaramappa Bootharaju ✉ ... See fewer authors ^

First published: 19 December 2023 | https://doi.org/10.1002/adma.202313032

❖Center for Nanoparticle Research, Institute for Basic Science (IBS), Seoul, 08826 Republic of Korea

❖School of Chemical and Biological Engineering Institute of Chemical Processes, Seoul National University, Seoul, 08826 Republic of Korea

❖School of Chemistry and Chemical Engineering Chongqing Key Laboratory of Theoretical and Computational Chemistry, Chongqing University, Chongqing, 401331 China

Angewandte International Edition Chemie

GDCh A Journal of the German Chemical Society

Angewandte Chemie International Edition homepage

Research Article

Homoleptic Alkynyl-Protected Ag_{15} Nanocluster with Atomic Precision: Structural Analysis and Electrocatalytic Performance toward CO_2 Reduction

Lubing Qin, Fang Sun, Xiaoshuang Ma, Guanyu Ma, Yun Tang, Dr. Likai Wang, Prof. Qing Tang, Prof. Rongchao Jin, Prof. Zhenghua Tang

First published: 24 September 2021 | https://doi.org/10.1002/anie.202110330 | Citations: 40

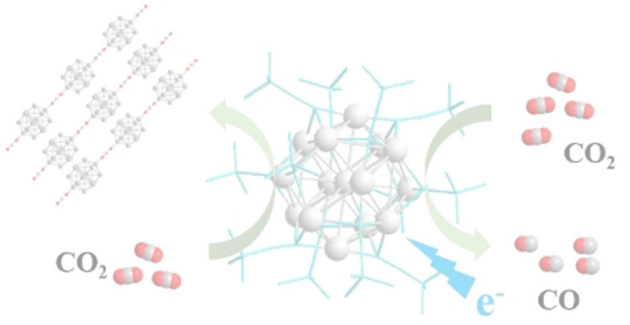

Homoleptic Alkynyl-protected Ag_{15} nanocluster for CO_2 reduction reaction

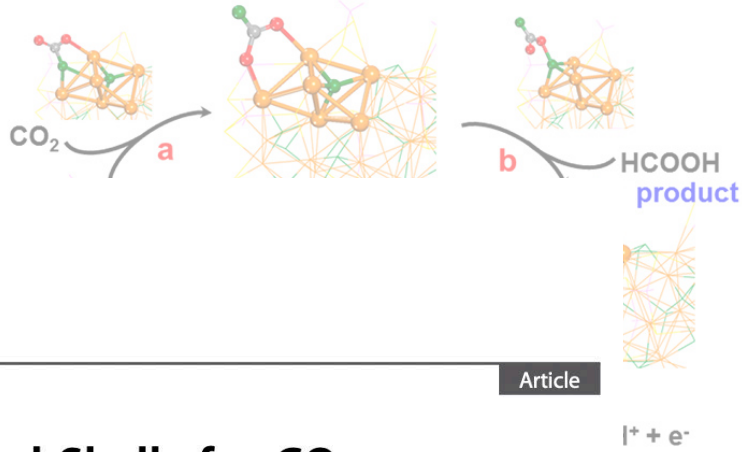

JACS

JOURNAL OF THE AMERICAN CH

Lattice-Hydride M
Structurally Preci

Qing Tang,† Yongjin Lee, and De-en Jiang*,†

CHEMISTRY OF MATERIALS

pubs.acs.org/cm

Article

Cu_{26} Nanoclusters with Quintuple Ligand Shells for CO_2 Electrocatalytic Reduction

Simin Li,⊥ Xiaodan Yan,⊥ Jiaqi Tang,⊥ Dongxu Cao,⊥ Xueli Sun,⊥ Guolong Tian, Xiongkai Tang, Huifang Guo, Qingyuan Wu, Jing Sun, Jinlu He,* and Hui Shen*

Cite This: *Chem. Mater.* 2023, 35, 6123–6132

Read Online

Introduction

- Two atomically precise Ag NCs were designed with identical sizes and different surface microenvironments. Specifically, through the development of an interfacial ligand-exchange (LE) reaction of aqueous thiolated Ag_{25} NCs with an aromatic thiol composed of a bulky alkyl group adjacent to metal binding site, we obtained organic-soluble Ag_{25} NCs with a well-defined surface microenvironment.
- These two model NCs enable us to study the role of local surface hydrophilicity and hydrophobicity in the eCO_2RR. The hydrophobic Ag_{25} cluster exhibits excellent eCO_2RR performance with >90% CO Faradaic efficiency (FE_{CO}) both in H-cell and membrane electrode assembly (MEA) device.
- On the other hand, Ag_{25} cluster with confined hydrophilicity exhibits only 66.6% FE_{CO} due to a distinct interfacial structure of water. Furthermore, the hydrophobic cluster exhibits high eCO_2RR activity with a CO partial current density (j_{CO}) of up to $-240\ mA\,cm^{-2}$ in an MEA device.
- Operando surface enhanced infrared absorption spectroscopy reveals the effect of the nature of ligand-shell on the interfacial structure of water, which plays vital role in the reaction kinetics. Furthermore, theoretical calculations support the experimental findings and reveal the critical role of confined surface microenvironment in eCO_2RR.

Captopril (Capt)

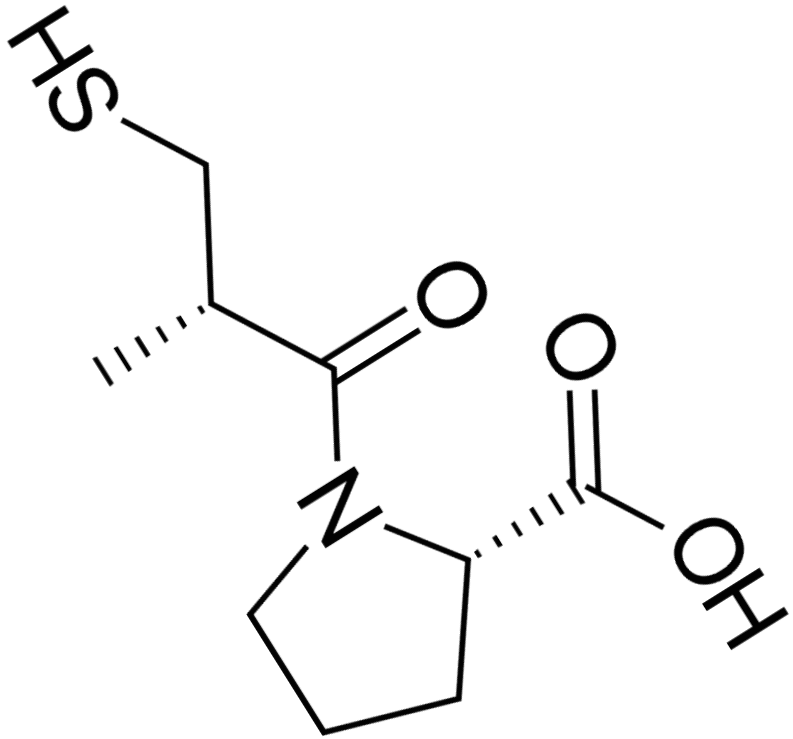

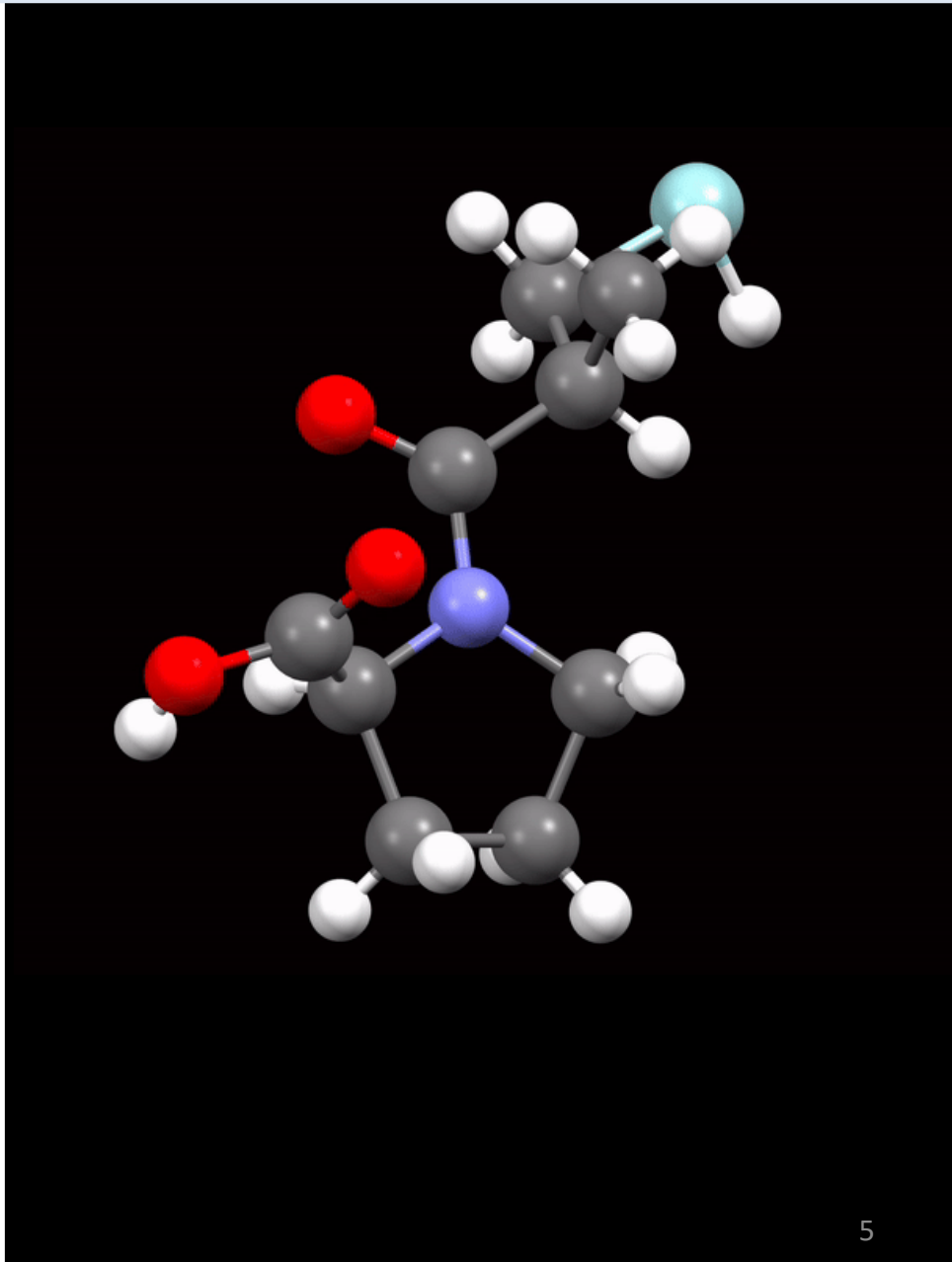

Captopril, sold under the brand name Capoten among others, is an angiotensin-converting enzyme (ACE) inhibitor used for the treatment of hypertension and some types of congestive heart failure. Captopril was the first oral ACE inhibitor found for the treatment of hypertension.

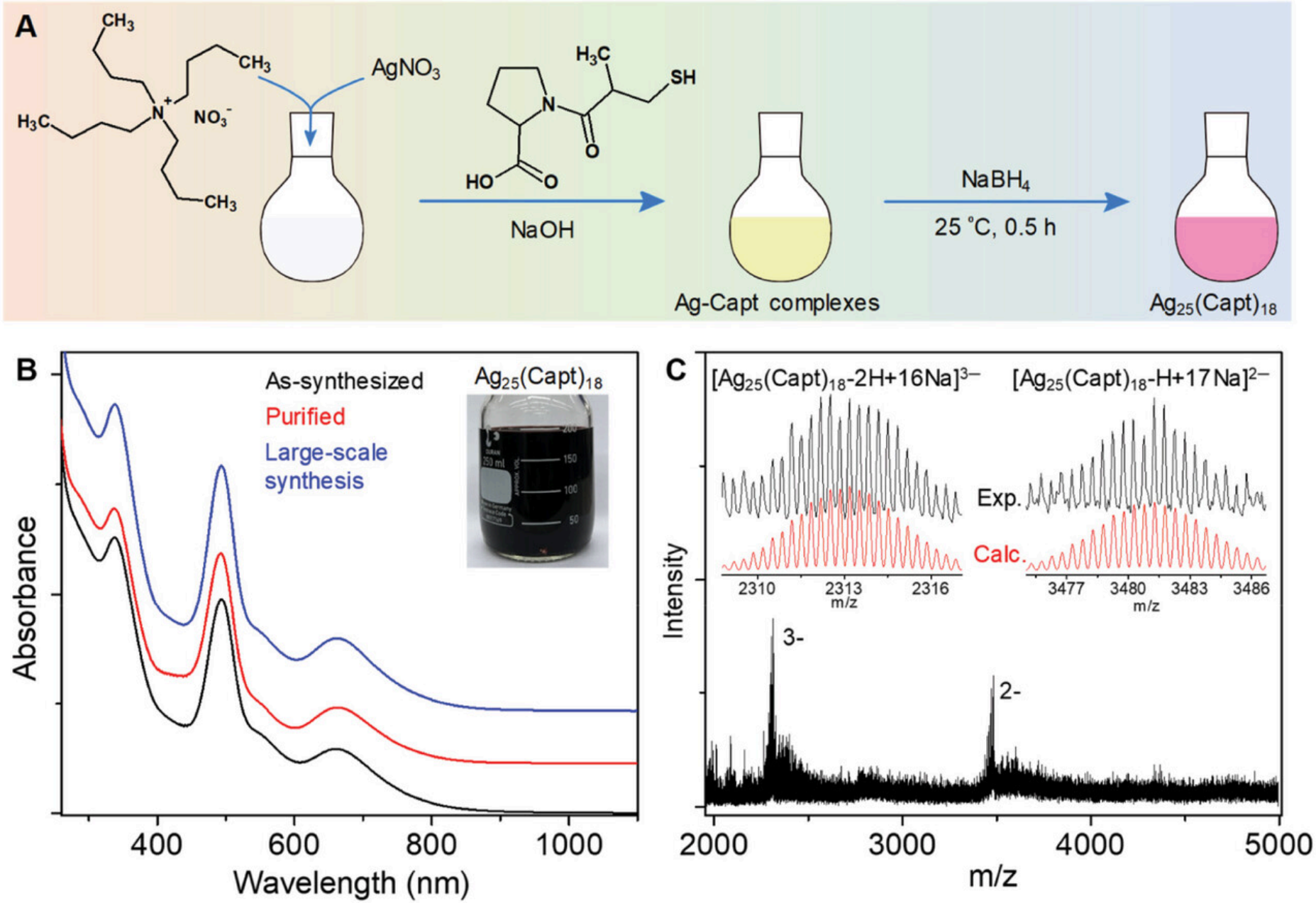

Figure 1 Synthesis and mass-characterization. A) Synthesis scheme of $[Ag_{25}(Capt)_{18}]^-$ NCs. B) Comparison of UV–vis absorption spectra of as-synthesized and purified NCs with that of the $[Ag_{25}(Capt)_{18}]^-$ NCs synthesized on a large scale (see inset). The red and blue spectra are vertically shifted for clarity. C) HR-ESI-MS of as-synthesized $[Ag_{25}(Capt)_{18}]^-$ NCs. Insets show the comparison of experimental (Exp.) and calculated (Calc.) mass spectra of displayed compositions.

Ligand exchange reaction at a hydrophilic-hydrophobic interface

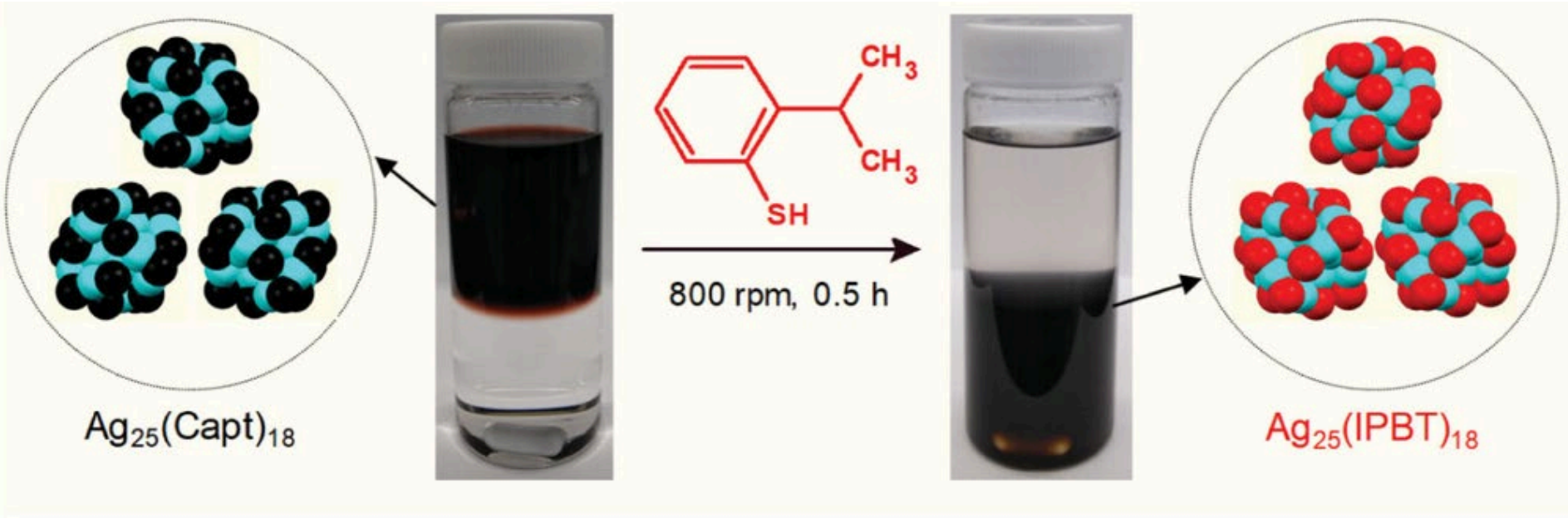

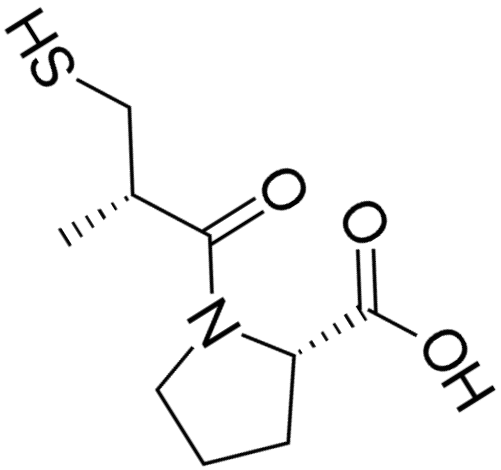

Captopril (Capt)

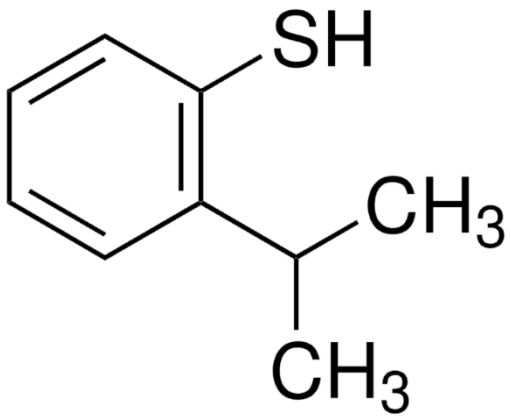

2-Isopropylbenzenethiol (IPBT)

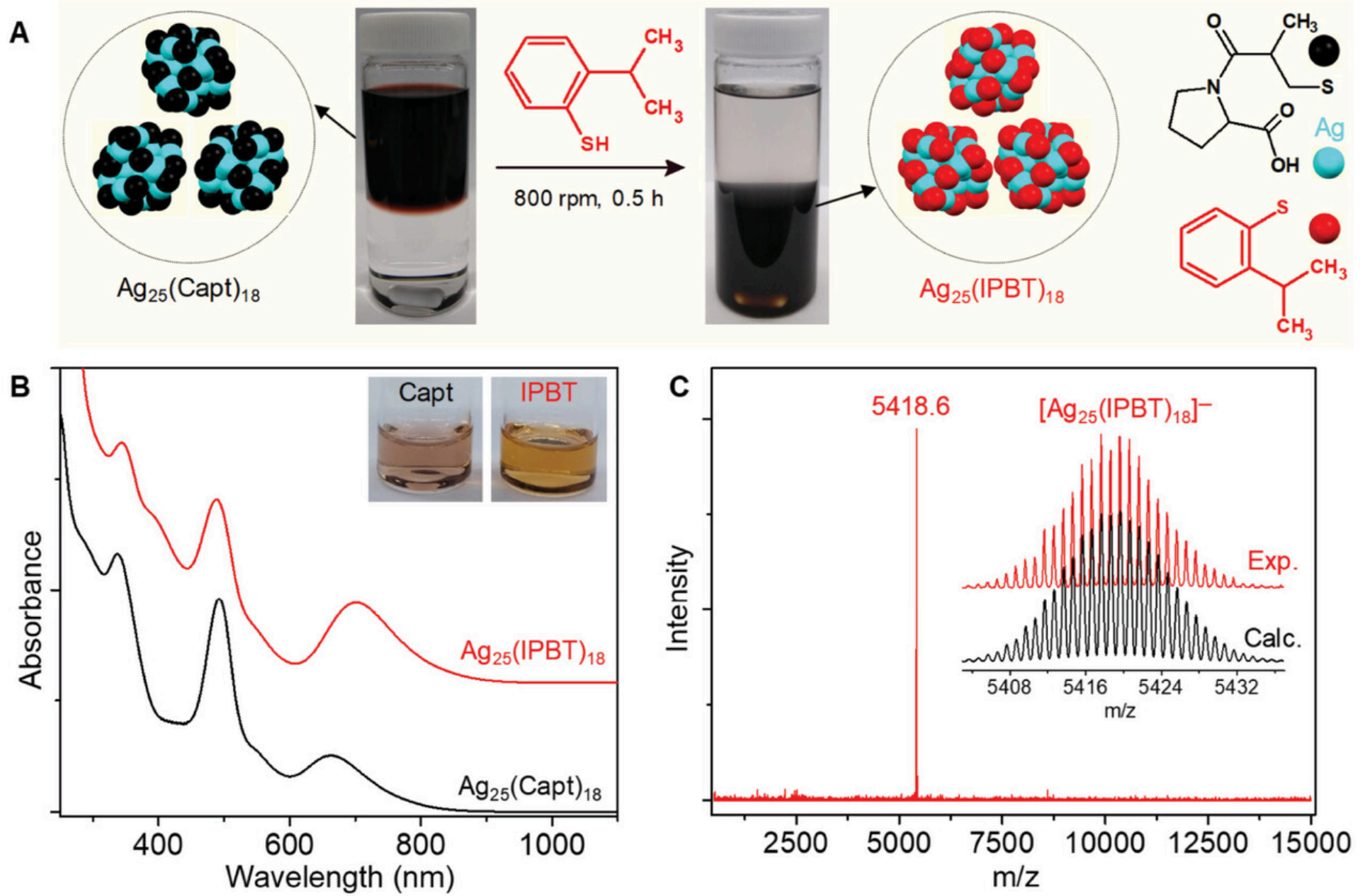

Figure 2 Size-preserved LE synthesis and mass-characterization. A) Biphasic LE synthesis scheme. Photographs show the biphasic separation of $[Ag_{25}(Capt)_{18}]^-$ NCs in water (left) and $[Ag_{25}(IPBT)_{18}]^-$ NCs in DCM (right). B) UV–vis absorption spectra of $[Ag_{25}(Capt)_{18}]^-$ NCs and LE product $[Ag_{25}(IPBT)_{18}]^-$ NCs. The red trace is vertically shifted for clarity. Insets show the photographs of respective NC solutions. C) HR-ESI-MS of $[Ag_{25}(IPBT)_{18}]^-$ NCs synthesized through LE. Inset shows the comparison of Exp. and Calc. mass spectra of [Ag25(IPBT)18]$^-$.

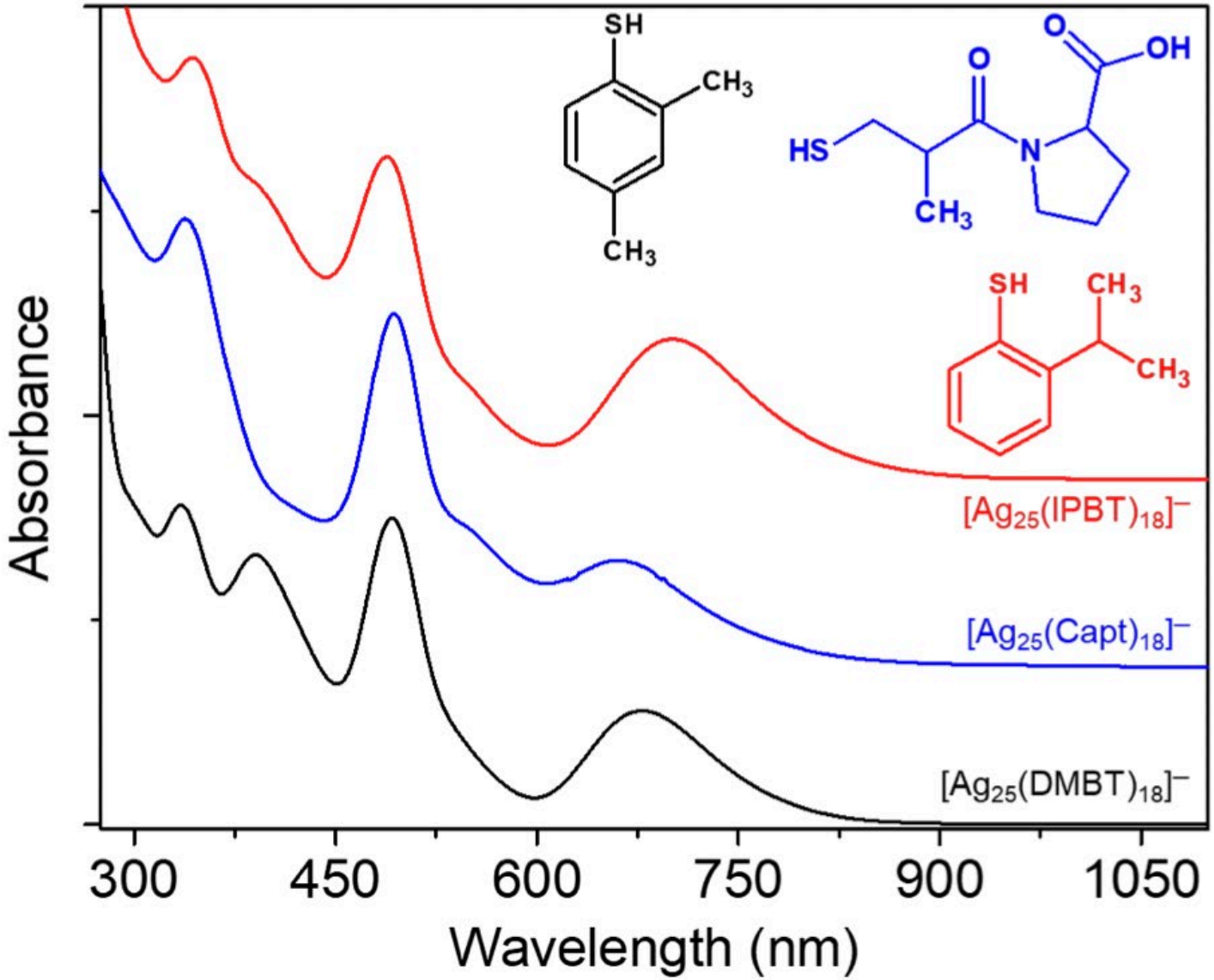

UV-vis absorption spectra of $[Ag_{25}(IPBT)_{18}]^{-}$, $[Ag_{25}(DMBT)_{18}]^{-}$ and $[Ag_{25}(Capt)_{18}]^{-}$ clusters. Insets show the molecular structures of respective thiol ligands.

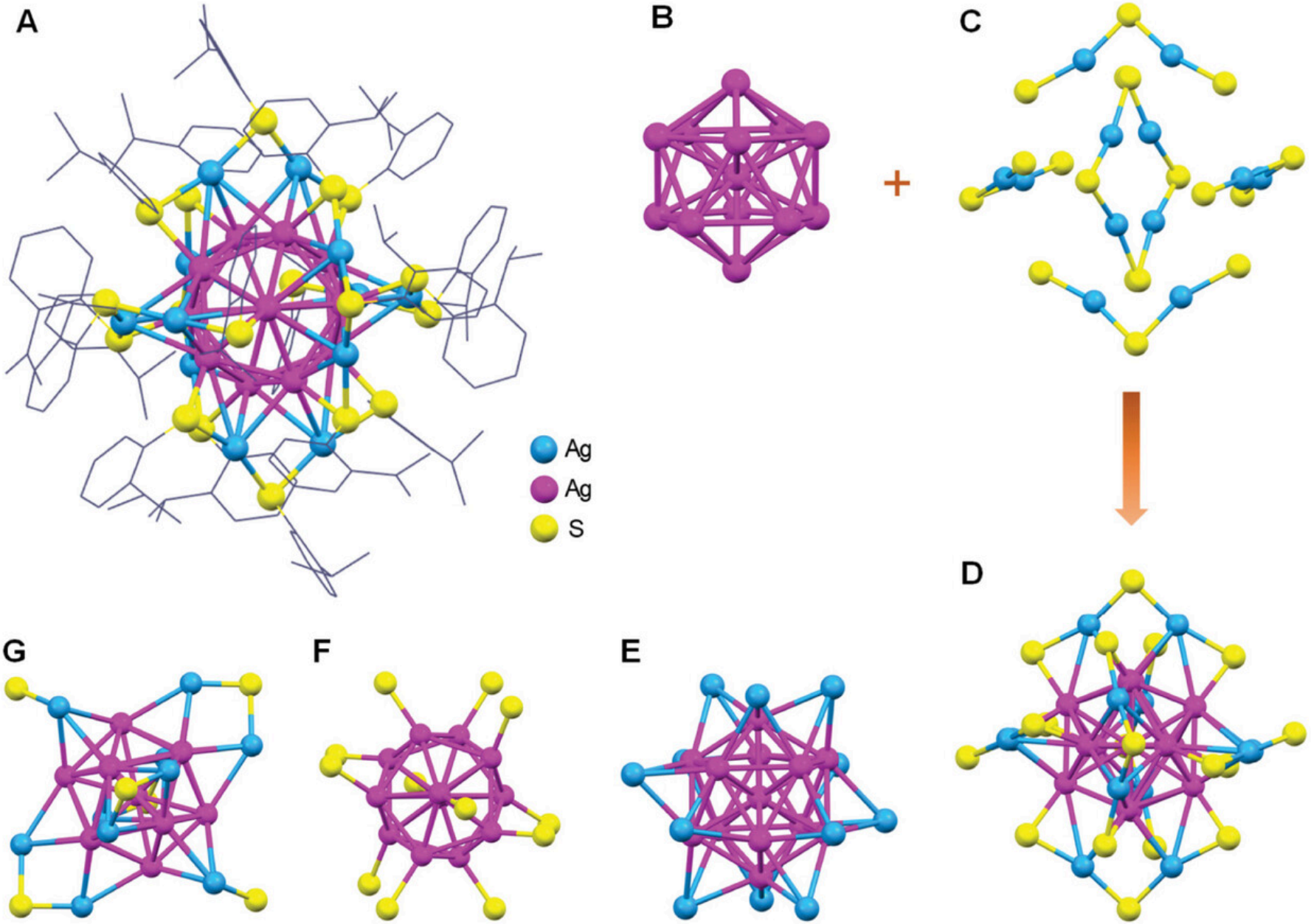

Analysis of the atomic-level structure obtained from SCXRD data. A) Total molecular structure of $[Ag_{25}(IPBT)_{18}]^-$ NC. B) Ag_{13} icosahedron core and C) six equivalent $Ag_2(IPBT)_3$ motifs. D) Formation of the structure of $[Ag_{25}(IPBT)_{18}]^-$ by capping the Ag_{13} core with motifs in C. E) Ag_{25} framework without thiolates. F) Thiolate-bound Ag_{13} core. G) Ag_{25} with thiolate-free Ag_{13} core. Carbon and hydrogen atoms of IPBT ligand are omitted in (C–G) for clarity.

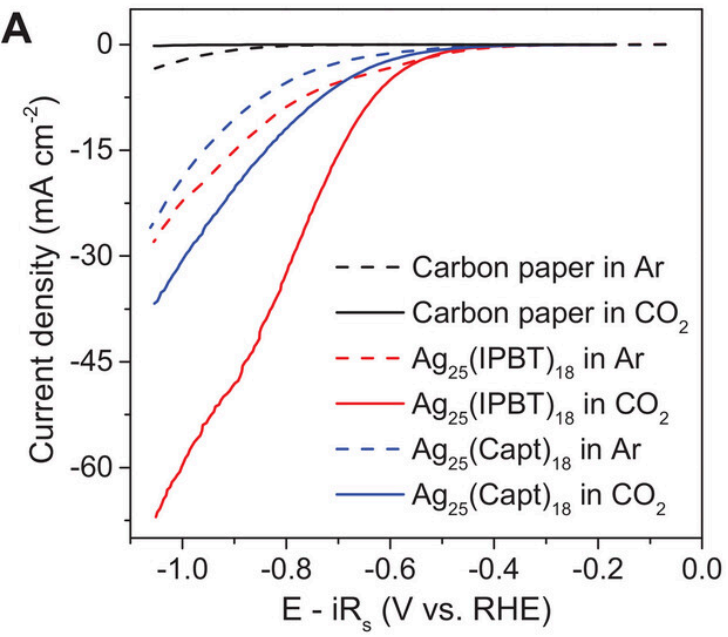

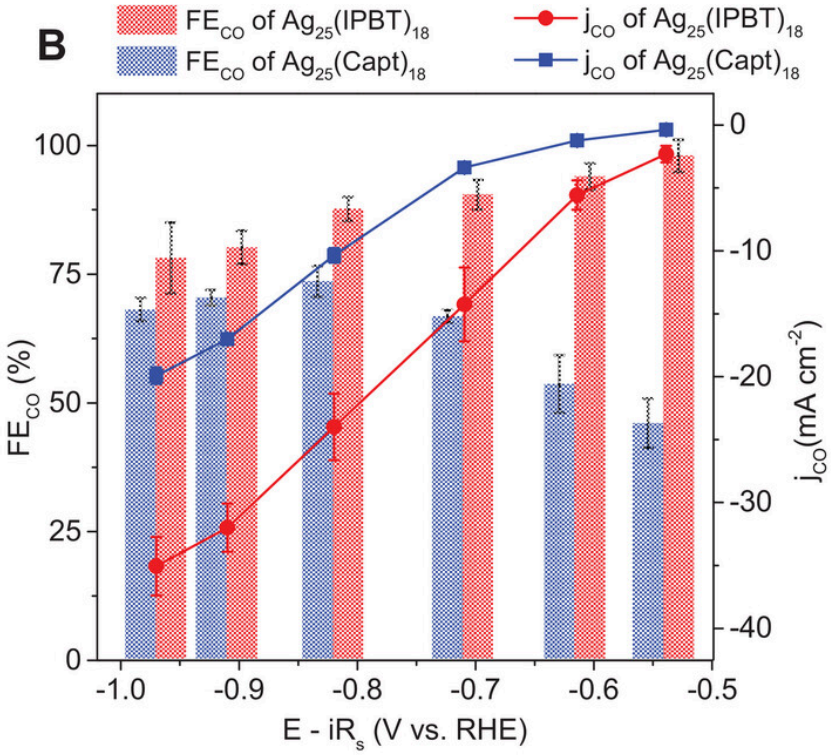

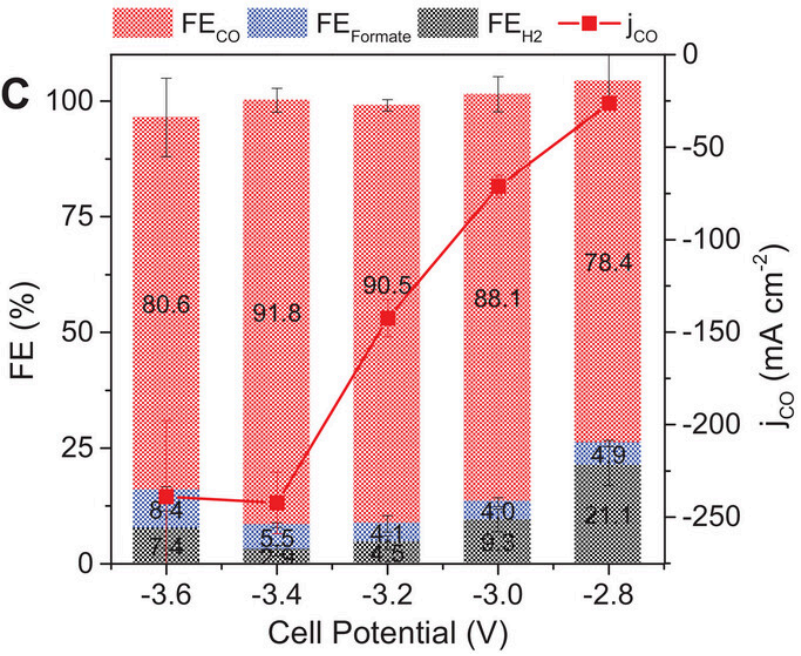

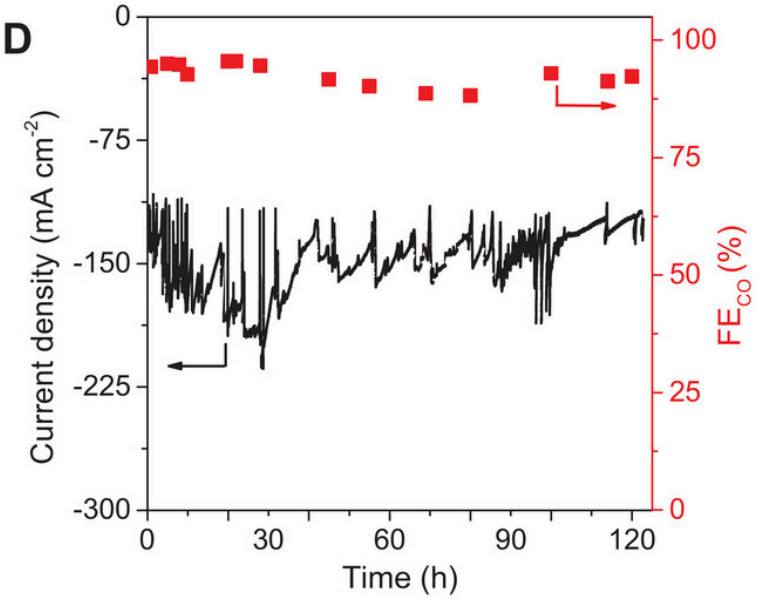

CO2 electroreduction. A) Polarization curves of $Ag_{25}(IPBT)_{18}$ and $Ag_{25}(Capt)_{18}$ in Ar- and CO2- saturated 0.5 mKHCO3. B) FE_{CO} and j_{CO} of $Ag_{25}(IPBT)_{18}$ and $Ag_{25}(Capt)_{18}$ in the potential range from −0.54 to −0.97 VRHE in the H-cell. C) FE_{CO} and j_{CO} of $Ag_{25}(IPBT)_{18}$ in the cell potential range from −2.8 to −3.6 V in the MEA cell. D) Long-term operation of $Ag_{25}(IPBT)_{18}$ at −3.2 V cell potential in the MEA cell. The error bars in (B) and (C) indicate the standard deviation of three independent experiments.

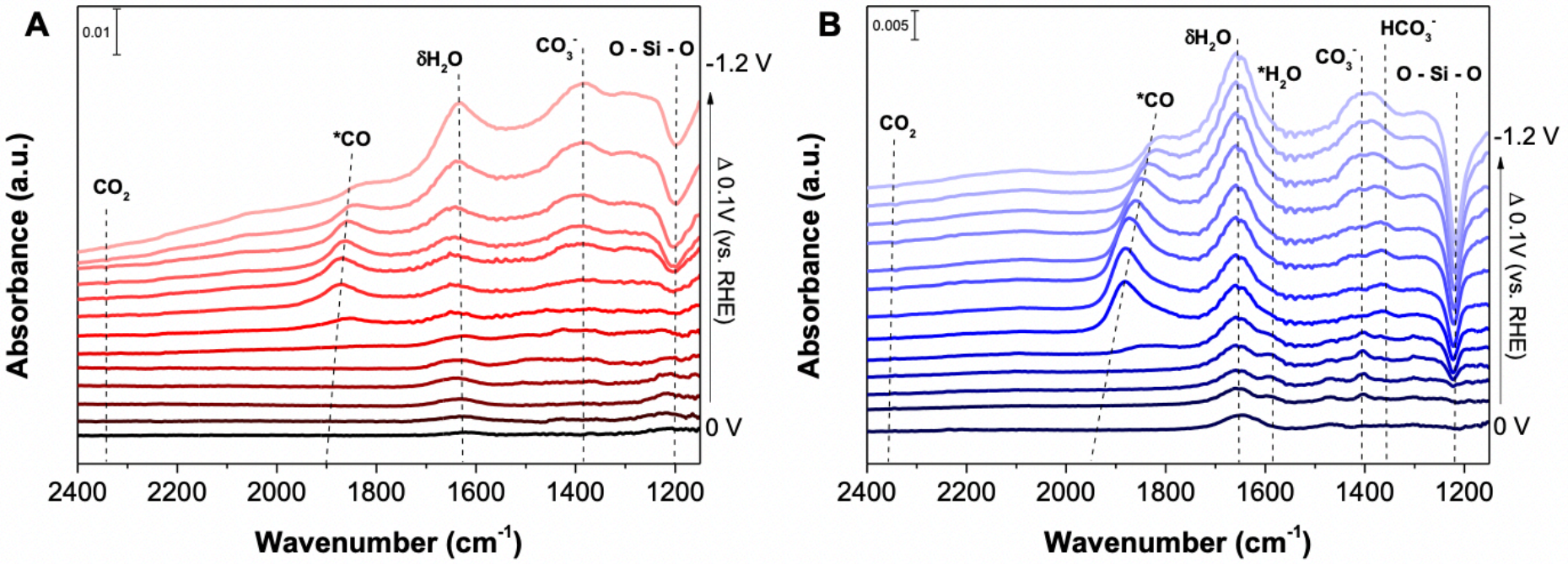

Full-range operando ATR-SEIRAS spectra on (A) $[Ag_{25}(IPBT)_{18}]^-$ and (B) $[Ag_{25}(Capt)_{18}]^-$ clusters during eCO_2RR.

ATR-SEIRAS stands for attenuated total reflectance surface-enhanced infrared absorption spectroscopy. It is a surface-sensitive technique similar to surface-enhanced Raman spectroscopy (SERS).

ATR-SEIRAS uses a silicon prism with one surface coated with a thin (~30 nm) metal film. Infrared light passes through the prism and is totally internally reflected. The evanescent wave excites surface plasmon polaritons at the metal/ air interface.

The increased electric field is confined to the interface, so absorption probabilities of surface molecules increase by an order of magnitude or more!

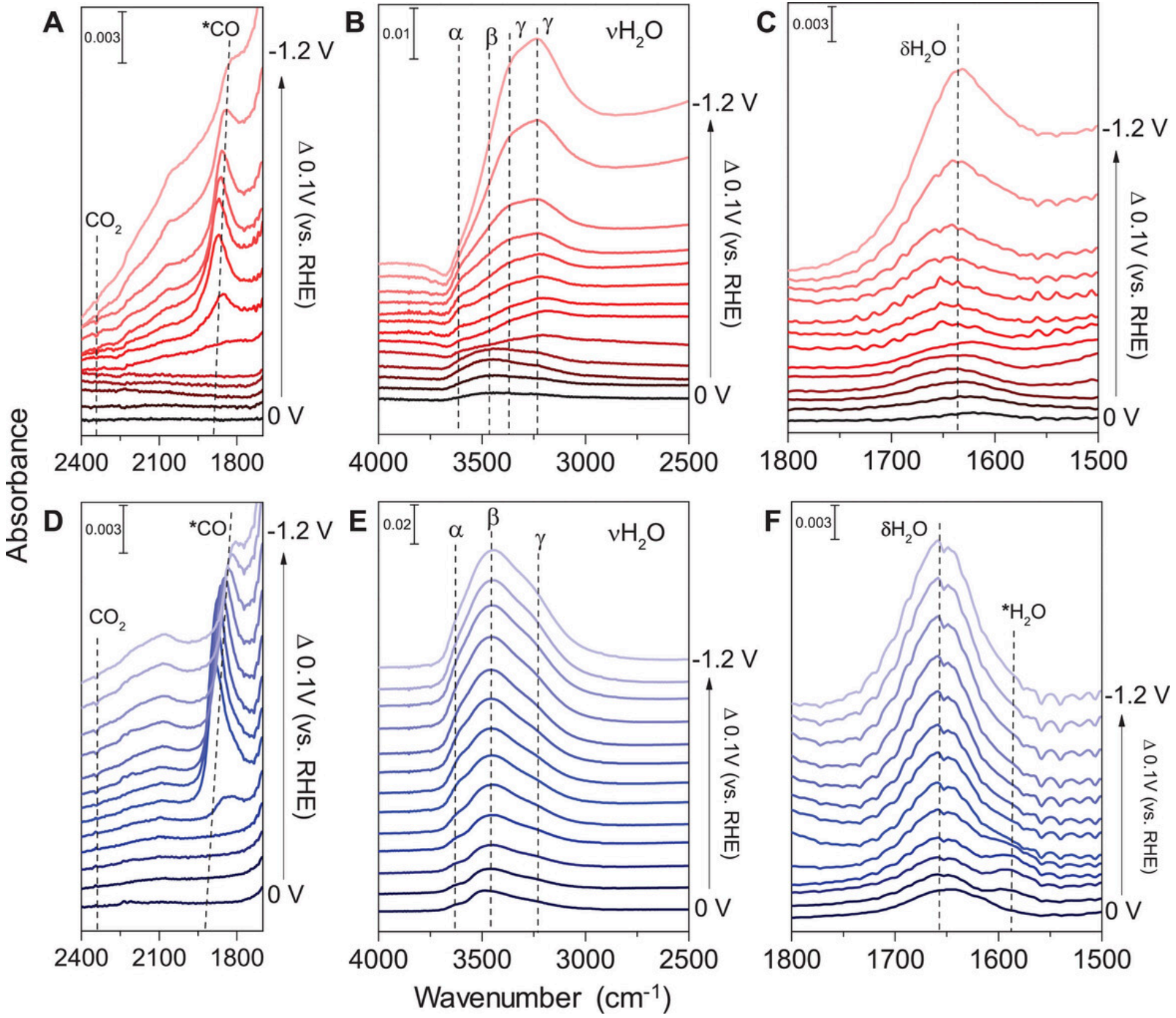

Operando spectroscopy. Operando ATR-SEIRAS spectra collected in the CO_2-saturated 0.5 m $KHCO_3$ electrolyte with 0.1 V intervals from 0.0 to −1.2 V_{RHE} on A–C) $Ag_{25}(IPBT)_{18}$ and D–F) $Ag_{25}(Capt)_{18}$. Full-range spectra in Figure S12, Supporting Information are shown as three separate parts: A,D) *CO, B,E) νH_2O, and C,F) δH_2O. Here, *denotes catalyst surface. The symbols in Figure 5 are not reproduced as in original Figure 5. Please correct them as per provided Figure 5.

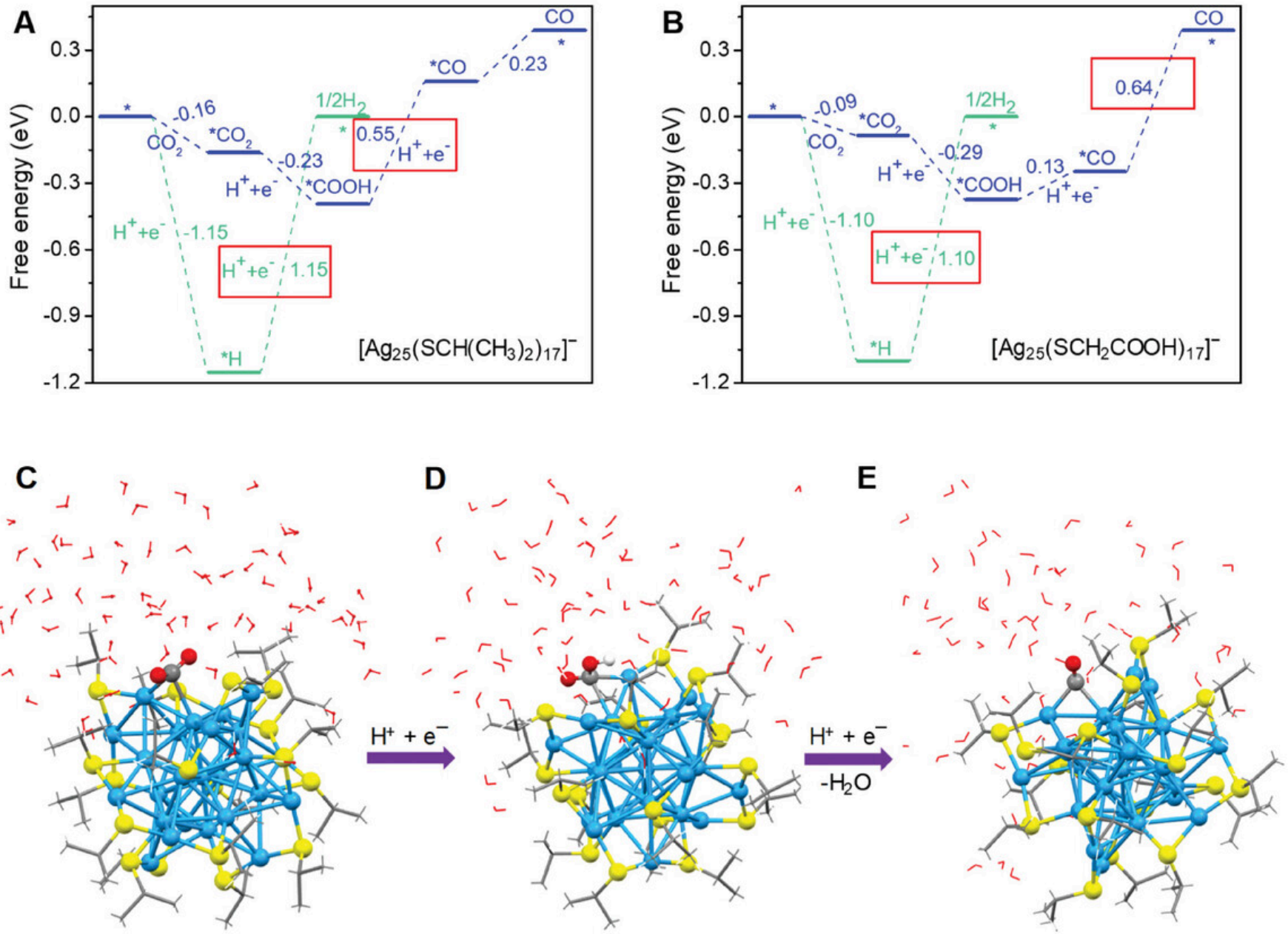

Theoretical analysis of eCO_2RR. Comparison of the free energy change of eCO_2RR to CO versus HER on dethiolated A) $[Ag_{25}(SCH(CH_3)_2)_{17}]^-$ and B) $[Ag_{25}(SCH_2COOH)_{17}]^-$ clusters at zero applied potential. The PDS of the reaction is framed in red. C–E) Optimized structures of the reaction intermediates, C) *CO2, D) *COOH, and E) *CO adsorbed on the surface of dethiolated $[Ag_{25}(SCH(CH_3)_2)_{17}]^-$ cluster exposed to H_2O molecules. Here, *denotes catalyst surface. Color legend: Ag, blue; S, yellow; C, gray; O, red; H, white.

Conclusion

- We present the design and large-scale synthesis of two atomically precise Ag_{25} NCs protected with thiolate ligands that create different local microenvironments, one with hydrophobicity and the other with hydrophilicity.
- Specifically, the hydrophobic Ag_{25} cluster exhibits remarkable selectivity for CO (>90%) and achieves a high current density of up to $-240\ mA\ cm^{-2}$ with excellent durability lasting for more than 120 h.
- Operando ATR-SEIRAS and theoretical calculations are utilized to gain atomistic insights into the crucial role of the ligand type in CO_2 electroreduction.
- The superior performance of the hydrophobic Ag_{25} cluster underscores the importance of its tailored surface microenvironment in enhancing intrinsic CO_2 reduction activity by decreasing the interaction with the water molecules. These results have valuable implications for the development of efficient and selective catalysts for CO_2 conversion, contributing to the advancement of sustainable energy technologies.